

Stereodivergent $S_N2@P$ Reactions of Borane Oxazaphospholidines: Experimental and Theoretical Studies

Hester Zijlstra,^{†,⊥} Thierry León,^{‡,⊥} Abel de Cózar,[†] Célia Fonseca Guerra,[†] Daniel Byrom,[‡] Antoni Riera,^{*,‡,§} Xavier Verdaguer,^{*,‡,§} and F. Matthias Bickelhaupt^{*,†,||}

[†]Department of Theoretical Chemistry, Amsterdam Center for Multiscale Modeling (ACMM), VU University Amsterdam, De Boelelaan 1083, NL-1081 HV Amsterdam, The Netherlands

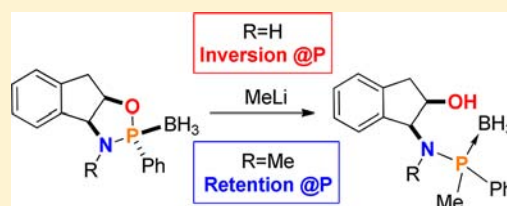
[‡]Institute for Research in Biomedicine (IRB Barcelona), C/Baldiri Reixac 10, E-08028 Barcelona, Spain

[§]Departament de Química Orgànica, Universitat de Barcelona, Martí i Franqués, 1, E-08028 Barcelona, Spain

^{||}Institute of Molecules and Materials, Radboud University Nijmegen, Heyendaalseweg 135, NL-6525 AJ Nijmegen, The Netherlands

Supporting Information

ABSTRACT: The stereodivergent ring-opening of 2-phenyl oxazaphospholidines with alkyl lithium reagents is reported. N-H oxazaphospholidines derived from both (+)-*cis*-1-amino-2-indanol and (–)-norephedrine provide inversion products in a highly stereoselective process. In contrast, N-Me oxazaphospholidines yield ring-opening products with retention of configuration at the P center, as previously reported by Jugé and co-workers. As a result, from a single amino alcohol auxiliary, both enantiomers of key P-stereogenic intermediates could be synthesized. Theoretical studies of ring-opening with model oxazaphospholidines at the DFT level have elucidated the stereochemical course of this process. N-H substrates react in a single step via preferential backside $S_N2@P$ substitution with inversion at phosphorus. N-methylated substrates react preferentially via a two-step frontside $S_N2@P$, yielding a ring-opened product in which the nucleophilic methyl binds to P with retention of configuration. DFT calculations have shown that the BH_3 unit is a potent directing group to which the methyl lithium reagent coordinates via Li in all the reactions studied.

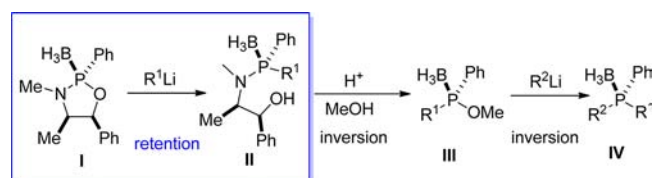


1. INTRODUCTION

Chiral phosphines have played a crucial role in the emergence of asymmetric metal catalysis as an efficient tool to produce single-enantiomer compounds.¹ One of the historical contributions in this field was the development of the P-stereogenic phosphine ligands PAMP and DIPAMP and their application in asymmetric hydrogenation for the synthesis of the anti-alzheimer drug L-DOPA.² Today, P-stereogenic phosphines attract increasing interest from the asymmetric catalysis community because of their capacity to impart excellent selectivities.^{3,4} However, the methods for the synthesis of these compounds are scarce and limited in terms of substrate scope. One of the most well-established approaches for the synthesis of P-stereogenic ligands is the so-called “Jugé–Stephan method”, which is based on the nucleophilic ring-opening of ephedrine-derived borane oxazaphospholidines (BOPs) in an $S_N2@P$ process with alkyl lithium reagents (Scheme 1).^{5,6} The main drawback of this strategy is that it is not amenable for the synthesis of bulky phosphines because of the lack of reactivity of intermediate II.⁷

Recently, we described that oxazaphospholidines are also amenable for the synthesis of bulky P-stereogenic aminophosphines.⁸ *tert*-Butyl oxazaphospholidine **1** derived from *cis*-1-amino-2-indanol (**3**) reacted stereoselectively with alkyl lithium or Grignard reagents to furnish the corresponding ring-opening products (Scheme 2). The presence of a free N-H

Scheme 1. Synthesis of P-Stereogenic Phosphines Using the Jugé–Stephan Method with Ephedrine^a



^aRing-opening of BOP highlighted in blue.

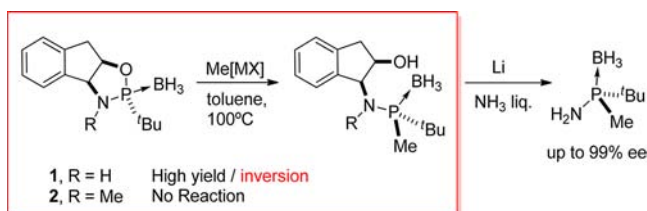
group in **1** was a key element for the success of the reaction. For example, N-methyl oxazaphospholidine **2** did not undergo ring-opening under the same reaction conditions (Scheme 2). Most noticeably, $S_N2@P$ of **1** took place with unprecedented inversion of configuration at the P center, while ring-opening in the ephedrine Jugé–Stephan system (Scheme 1) takes place with retention of configuration.⁵

The opposite stereochemical pathways observed for these two systems can be attributable to the following: (a) *tert*-butyl vs phenyl substitution at the 2 position of the BOP ring; (b) hydrogen vs methyl substitution at the N atom of the BOP ring; and (c) the use of distinct 1,2-amino alcohol scaffolds. To

Received: January 8, 2013

Published: February 25, 2013

Scheme 2. Synthesis of P-Stereogenic Aminophosphines Using (+)-*cis*-1-Amino-2-indanol^a



^aRing-opening of BOP highlighted in red.

shed light on these issues, we examined the effect of these three factors on the stereoselective $S_N2@P$ reactions of BOPs. Here we report on the ring-opening of 2-phenyl oxazaphospholidines and how N-substitution allows discrimination between inversion and retention pathways in a completely stereodivergent process. Also, for the first time, we conducted a computational mechanistic exploration of the $S_N2@P$ reactions between methyl lithium and various model BOPs to explain the stereoselectivity observed using relativistic density functional theory (DFT; see computational details).

2. EXPERIMENTAL RESULTS

2.1. Ring-Opening Experiments with 2-Phenyl Oxazaphospholidines. Since 2-phenyl BOPs undergo rapid ring-opening with organolithium reagents at low temperatures,⁵ we chose 2-phenyl oxazaphospholidines **4** and **5** derived from (1*S*, 2*R*)-(+)-*cis*-1-amino-2-indanol (**3**) to study the process (Scheme 3). Condensation of **3** with the bis(diethylamino)phenylphosphine provided the corresponding BOP **4** as a 10:1 mixture of diastereomers in 76% yield. The major diastereomer with the *R* configuration at the P center was obtained by crystallization in hexane/ CH_2Cl_2 mixtures.⁹ Diastereomerically pure (*R_P*)-**4** was easily alkylated by deprotonation with MeLi and reaction with iodomethane to yield the N-Me BOP (*R_P*)-**5** as a single diastereomer in excellent yield.

With BOPs **4** and **5** in hand, we proceeded to test their ring-opening with two alkyl lithium reagents, namely methyl lithium and *ortho*-anisyl lithium (*o*-AnLi), which are widely used in this type of chemistry. The reaction of **4** and **5** took place efficiently at -78 °C for both MeLi and *o*-AnLi (Table 1). In all cases, ring-opening occurred with complete stereoselectivity, as determined by 1H NMR spectroscopy, to yield substitution compounds as single diastereomers. At this stage, the stereochemistry of compounds **6a–b** and **7a–b** could not be ascertained by X-ray analysis because these compounds either were oils or did not provide suitable crystals for analysis. However, we were able to undertake diffraction analysis for the methyl ether **9** obtained by permethylation of **6a** (Figure 1). The X-ray structure of this derivative (**9**) showed the P atom with the *S* configuration, thus confirming that $S_N2@P$ of **4** with MeLi took place with inversion of configuration at the P center in an analogous fashion, as happens with the *tert*-butyl BOP **1** (Scheme 2).

To fully ascertain the stereochemistry in the ring-opening of **4** and **5**, we next carried out the acid-catalyzed methanolysis of compounds **6a–b** and **7a–b** (Table 2). It is known that methanolysis of similar compounds takes place with inversion at the P center in a highly stereoselective manner.^{5a} The methanolysis of compounds **6a** and **7a**

Table 1. Ring-Opening of (+)-*cis*-1-Amino-2-indanol-Derived Phenyl Oxazaphospholidines

4, R = H, 5, R = Me
6, R = H, 7, R = Me

entry	S.M.	R	R'	yield (%)	dr ^a	product
1	4	H	Me	89	≥95:5	6a (<i>S_P</i>) ^c
2	5	Me	Me	89	≥95:5	7a (<i>R_P</i>) ^d
3	4	H	<i>o</i> -An ^b	73	≥95:5	6b (<i>R_P</i>) ^d
4	5	Me	<i>o</i> -An ^b	88	≥95:5	7b (<i>S_P</i>) ^d

^aDiastereomeric ratio was determined by 1H NMR spectroscopy. ^b*o*-An = *ortho*-anisyl (2-methoxyphenyl). ^cAbsolute configuration of dimethyl derivative **9** determined by X-ray analysis. ^dAbsolute configuration determined by analysis of the corresponding methanolysis product, see Table 2.

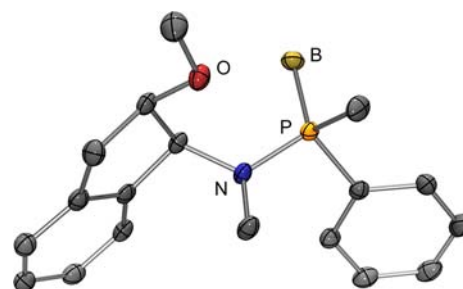


Figure 1. X-ray structure of methyl ether **9** prepared by permethylation of **6a** showing that the configuration at the phosphorus center is *S*.

provided the same methyl phosphinite **10** in high enantiomeric excess but with opposite configurations (Table 2, entries 1 and 2). A similar outcome was obtained for the methanolysis of phosphinoamines **6b** and **7b**. Compound **6b** led to dextrorotatory phosphinite **11**, while **7b** gave levorotatory phosphinite **11** (Table 2, entries 3 and 4). Therefore, the methanolysis of compounds **6** and **7** confirmed that the ring-opening of **4** and **5** occurs with high stereoselectivity but through opposite mechanistic pathways. Ring-opening of BOP **4**, which has a free N-H group, provides inversion, whereas the same reaction on BOP **5**, which contains an N-Me moiety, leads to retention of the configuration. As a result, from a single enantiomer of *cis*-1-amino-2-indanol auxiliary, both enantiomers of P-stereogenic phosphinites **10** and **11** could be synthesized.

To further confirm that the sole factor governing the stereodivergent ring-opening of BOPs is the substitution at the nitrogen atom and that the chiral auxiliary employed had no influence, we next studied the stereochemical course of the reaction using norephedrine derivatives (Scheme 4). Condensation of norephedrine with PhP(NEt_3)₂ in hot dioxane followed by protection with borane produced a mixture of diastereomers in an 8:1 ratio. Purification by flash chromatography yielded the major diastereomer (*R_P*)-**12** in 39%

Scheme 3. Synthesis of N-H and N-Me Phenyl Oxazaphospholidines Derived from (+)-*cis*-1-Amino-2-indanol

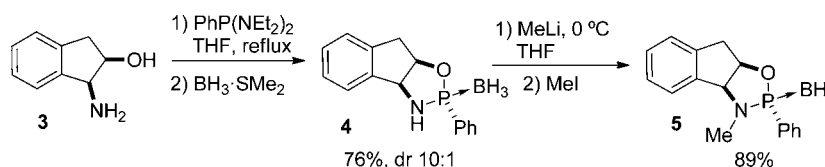
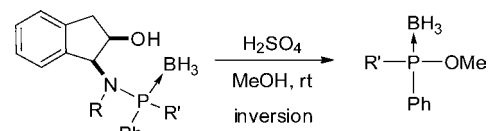


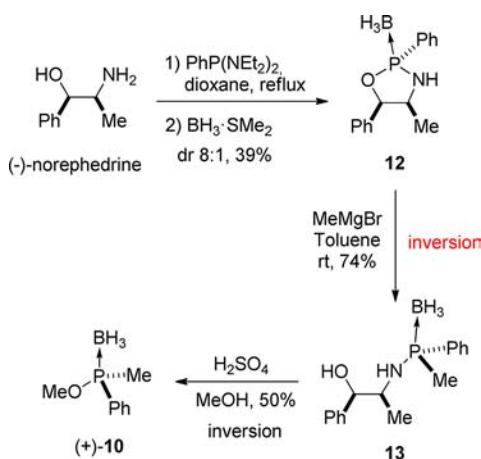
Table 2. Methanolysis of Aminophosphines 6a–b and 7a–b



entry	S.M.	R	R'	yield (%)	$[\alpha]_D^a$	ee (%) ^b	product ^c	stereochemical course ^d
1	6a	H	Me	89	+94.5	98	(+)-10-(R _p)	inver./inver.
2	7a	Me	Me	89	-94.4	98	(-)-10-(S _p)	ret./inver.
2	6b	H	<i>o</i> -An ^e	73	+26.9	99	(+)-11-(S _p)	inver./inver.
4	7b	Me	<i>o</i> -An ^e	88	-26.8	99	(-)-11-(R _p)	ret./inver.

^aOptical rotations were recorded in CHCl₃ at a concentration of 1g/100 mL. ^bEnantiomeric excess calculated on the basis of the optical rotations and data in the literature (ref 5a). ^cAbsolute configuration was determined on the basis of the sign of optical rotation (ref 5a). ^dStereochemical pathway observed for the ring-opening and methanolysis steps respectively. ^e*o*-An = *ortho*-anisyl (2-methoxyphenyl).

Scheme 4. Synthesis of Phosphinite 10 Using Norephedrine as a Chiral Auxiliary



yield.⁹ Treatment of **12** with MeMgBr at room temperature afforded the ring-opening product in >95:5 stereoselectivity, as determined by ¹H NMR. Finally, methanolysis of **13** provided dextrorotatory phosphinite (+)-(*R_p*)-**10** in 96% enantiomeric excess. These findings demonstrate that ring-opening for the norephedrine system takes place with inversion at the P center, as opposed to the known retention pathway observed for ephedrine.

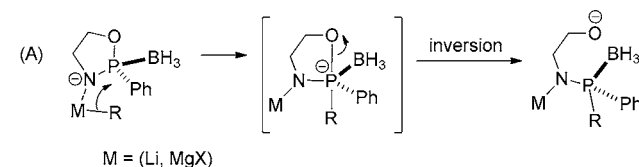
Overall, these results show that the only factor that regulates the stereodivergent ring-opening of oxazaphospholidines is the substitution at the nitrogen atom of the heterocycle. Thus, BOPs **4** and **12** bearing Ph and H substituents at P and N, respectively, react via backside *S_N2@P*, which is accompanied by inversion of configuration at the P center (Scheme 5A).⁸ Methyl substitution at N blocks this route and diverts the reaction toward the frontside *S_N2@P* pathway, which implies the retention of configuration (Scheme 5B).^{5b,c,10} In the case of BOP **1** bearing *t*-Bu (instead of Ph) and H substituents at P and N, respectively, the system still reacts via backside *S_N2@P*, i.e., with inversion of configuration. This time, however, methylation of N (**2**) not only blocks the backside pathway but also leaves the frontside *S_N2@P* route inaccessible. In this case, backside *S_N2@P* requires two equivalents of nucleophile to proceed, whereas frontside *S_N2@P* involves the usual one equivalent of organometallic reagent.

3. COMPUTATIONAL MECHANISTIC STUDIES

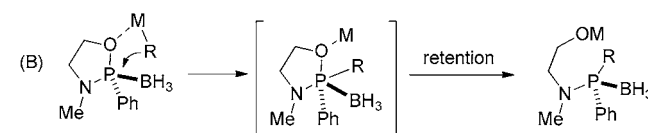
3.1. Computational Details. All calculations have been performed using the Amsterdam Density Functional (ADF) program¹¹ using DFT at OLYP/TZ2P for geometry optimization and energies.¹² TZ2P is a large uncontracted set of Slater-type orbitals (STOs) of triple- ζ quality for all atoms and was augmented with two sets of polarization functions, that is, p and d functions for the hydrogen atom and d and f functions for the other atoms. An auxiliary set of s, p, d, f,

Scheme 5. Postulated Reaction Pathways for the Ring-Opening of N-Me and N-H Borane Oxazaphospholidines

Backside *S_N2@P*



Frontside *S_N2@P*



and g STOs was used to fit the molecular density and to represent the Coulomb and exchange potentials accurately in each self-consistent field cycle. Relativistic effects were taken into account using the zeroth-order regular approximation (ZORA).¹³

Reactions were modeled both in the gas phase and in toluene, using methyl lithium as nucleophilic reagent, and the four borane oxazaphospholidines (BOPs) are depicted in Figure 2. Solvation in toluene has been simulated using the conductor-like screening model (COSMO).¹⁴

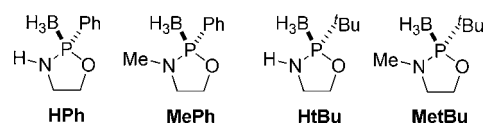


Figure 2. Model BOPs in this computational study.

In general, transition states (TSs) were determined by following the eigen mode with the negative force constant toward the saddle point on the potential energy surface. The following six TSs were determined by a linear transit (LT) in which the nucleophile–substrate C–P bond length varies from its values in the initial minimum to that in the final minimum, while optimizing all other geometry parameters in each LT point: postTS in backside *S_N2@P* of MePh in the gas phase and in toluene; TS in frontside *S_N2@P* of both HPh and of HtBu in the gas phase and in toluene. This procedure was shown before to yield excellent agreement with reaction profiles from steepest-descent computations.¹⁵ An LT approach was also used for determining the TS for the facile lithiation of HPh and HtBu. All stationary points were verified to be minima (zero imaginary frequencies) or TSs (one imaginary frequency) through vibrational analysis. The character of the mode representing the transition vector was examined, and attention was paid to a correct coupling of C–P

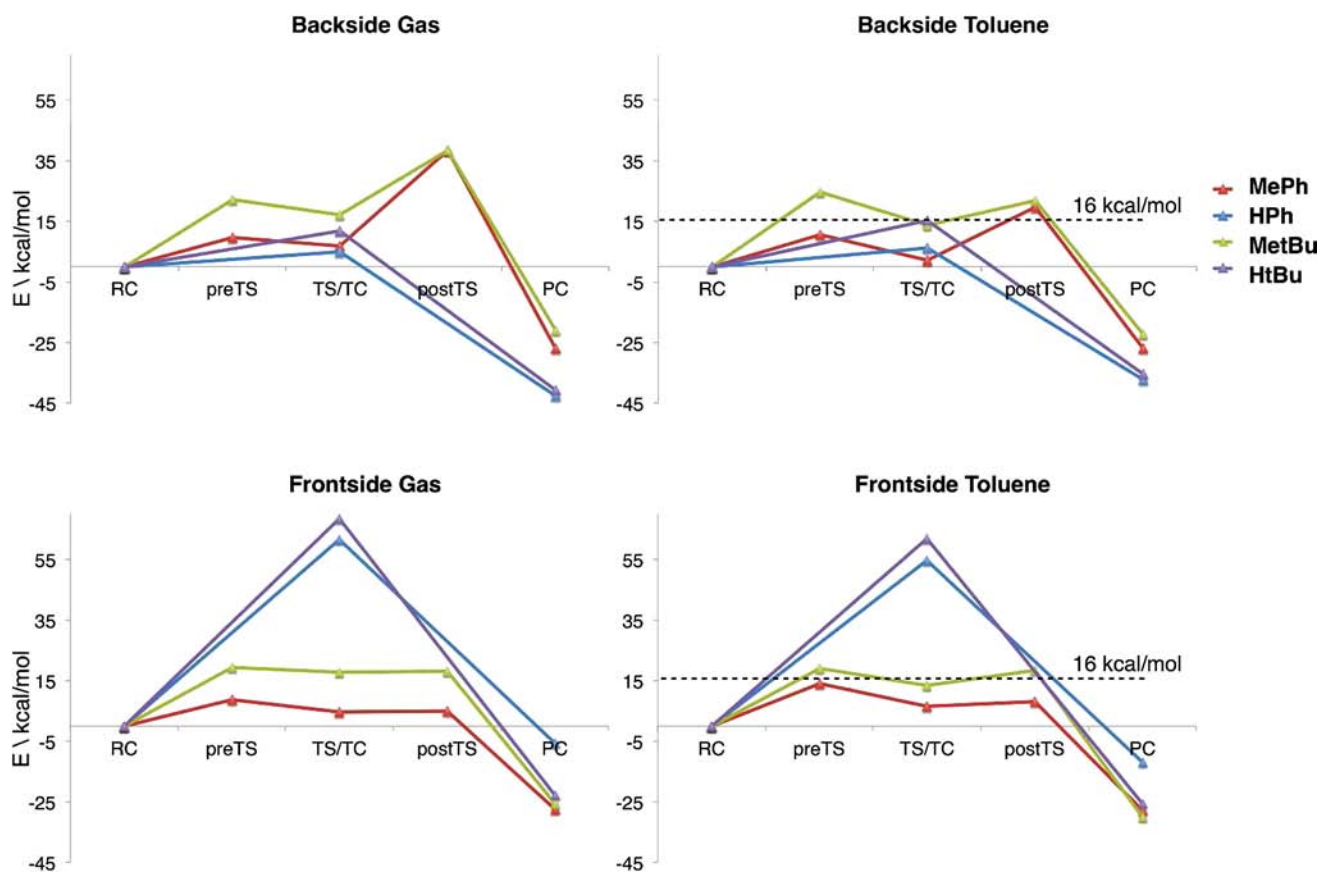


Figure 3. Reaction profiles of backside and frontside $S_N2@P$ reactions of MeLi + HPh, MePh, HtBu, and MetBu in the gas phase and in toluene, computed at (COSMO) ZORA-OLYP/TZ2P.

bond formation, P–O bond breaking, and Li^+ migration in the $S_N2@P$ TSs. In a few cases, species had a spurious imaginary frequency associated with nearly free rotation of methyl groups (see Supporting Information).

The electronic structure of key species was analyzed using quantitative Kohn–Sham molecular orbital (MO) theory.¹⁶ Furthermore, the electronic charge density distribution was evaluated using the Voronoi deformation density (VDD) atomic charge method.¹⁷

3.2. Overview of Mechanistic Pathways. Figure 3 shows our computed reaction profiles for the backside and frontside $S_N2@P$ reactions of methyl lithium with the four BOP substrates shown in Figure 2, in the gas phase and in toluene. A complete account of all structural data can be found in the Supporting Information. Relative energies of stationary points are specified with respect to the reactant complex (RC) that is formed prior to the substitution process, which occurs either in one step via a single TS or in two steps via a stable intermediate transition complex (TC) that is separated from the RC and the product complex (PC) by a pre- (preTS) and a post-transition states (postTS).

In the presence of methyl lithium,¹⁸ substrates HPh and HtBu undergo facile deprotonation at nitrogen under formation of the N-lithiated species + methane. For MeLi + HPh, this reaction is exothermic by -53.6 kcal/mol and proceeds via a barrier of <1 kcal/mol. A second methyl lithium molecule is then required to enter the nucleophilic substitution pathways.

The corresponding lithiation reaction is blocked in the case of the N-methylated substrates MePh and MetBu in which case already the first methyl lithium molecule can enter into the nucleophilic substitution pathways. This finding matches with the experimental observation that reactions involving N-methylated substrates proceed with only 1 equiv of methyl lithium, whereas unmethylated substrates require 2 equiv of methyl lithium.

Inspection of the condensed-phase reaction profiles shows that N-methylation raises the backside but not the frontside $S_N2@P$ barriers, whereas replacing the phenyl substituent at P by *t*-butyl raises both the backside and the frontside $S_N2@P$ barriers (see Figure 3). This is in line with earlier findings that increasing steric congestion near the electrophilic center causes higher S_N2 barriers.¹⁵ Interestingly, N-methylation goes for all model systems with a two-step substitution mechanism that involves a stable $S_N2@P$ TC, i.e., a stable pentacoordinate phosphorus intermediate, instead of a labile $S_N2@P$ TS. On the other hand, when the N atom carries a hydrogen, the substitution reactions proceed in a concerted (one-step) fashion. We will return to this later on.

Comparison of our computed reaction profiles with experimental data reveals that model reactions in toluene that involve TSs >16 kcal/mol relative to the reactant complex do not occur in the experiments (compare Figure 3 with Schemes 1 and 2). There are three model reactions in which no TS higher than 16 kcal/mol relative to the reactant complex occurs: 2 MeLi + HPh via b- $S_N2@P$; 2 MeLi + HtBu via b- $S_N2@P$; and MeLi + MePh via f- $S_N2@P$ (see Figure 3). This agrees well with the experimental finding that BOP substrates carrying hydrogen at N react via backside $S_N2@P$, N-methylated substrates with phenyl-substitution at P react via frontside $S_N2@P$, and simultaneous N-methylation and *t*-butyl substitution at P make substrates unreactive.

3.3. Reactions of MePh. Figure 4 compares the energy profiles of backside and frontside $S_N2@P$ reactions of MeLi + MePh, starting from the reactant complexes. The energy of stationary points is again shown relative to the reactant complex. Both pathways show the two-step mechanism that is usual for S_N2 at phosphorus and other third- and higher period electrophilic centers.^{15,19}

The BH_3 group at phosphorus acts as a directing group to which the metal-stabilized nucleophile MeLi coordinates via lithium (see Scheme 6).¹⁰ In this way, the methyl anion is effectively positioned for

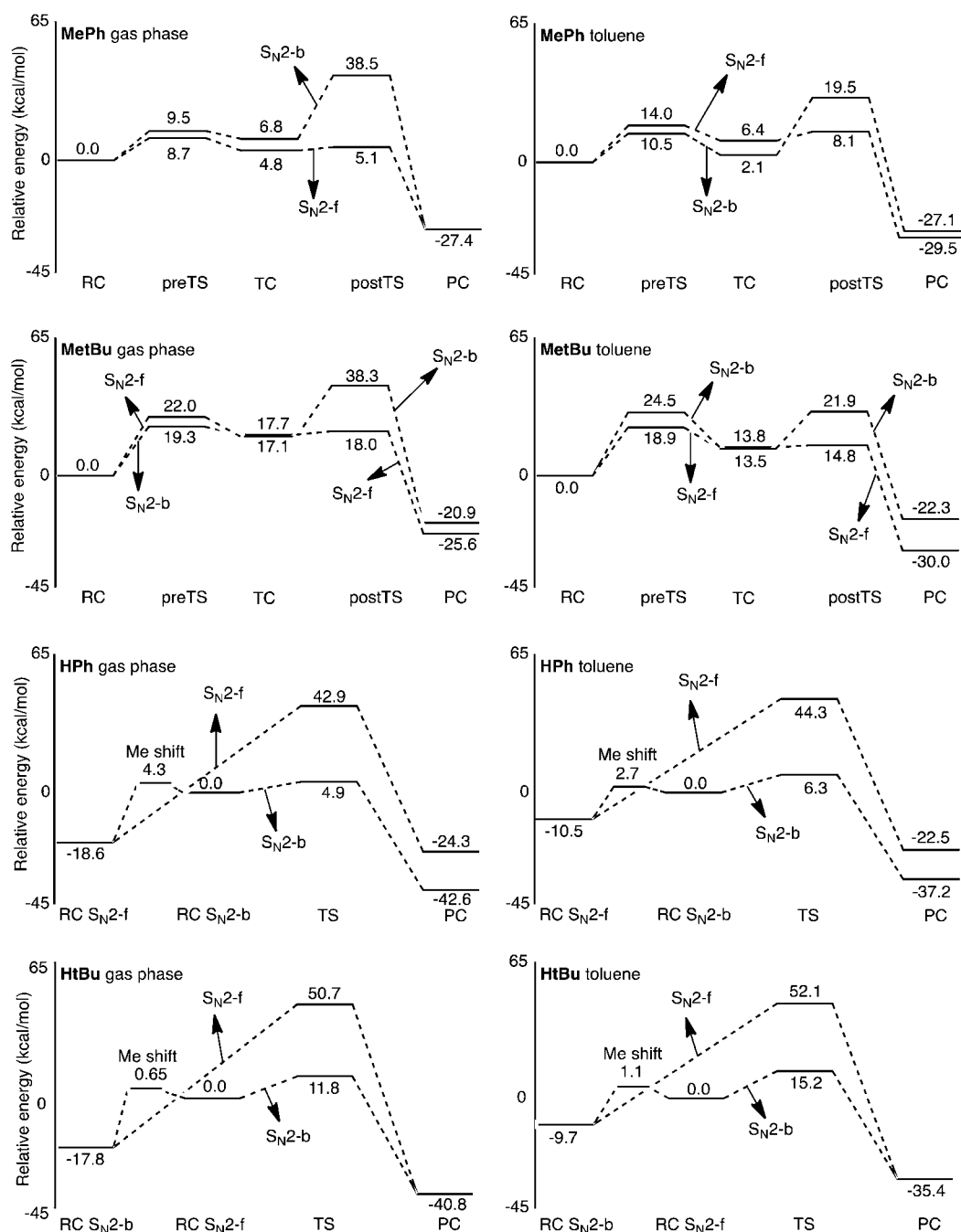
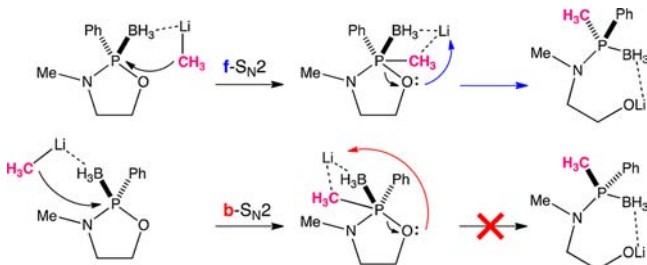


Figure 4. Backside versus frontside S_N2@P reaction profiles for each of our four substrates in the gas phase and in toluene, computed at (COSMO) ZORA-OLYP/TZ2P.

Scheme 6. Computed Backside and Frontside S_N2@P Pathways of MeLi + MePh



nucleophilic attack, both in the backside and frontside S_N2@P mechanism. In the course of the first elementary step, this leads to the formation of the pentacoordinate TC, in which the BH₃ group hosts and stabilizes the lithium cation that is released as the methyl anion forms a new bond with phosphorus.

A critical factor in the second elementary step (i.e., dissociation of the P–O bond) is the feasibility of stabilizing the evolving alkoxide leaving group by the lithium cation. In both, backside and frontside S_N2@P pathways, the associated postTS possesses a transition vector in which Li moves from P toward O, while simultaneously the P–O bond is dissociating. In the TC of the backside process (b-MePh-TC), the ~0.6 Å longer Li–O distance (see Figure 5) leads to a high barrier in the second reaction step (see Figure 4). In the frontside pathway, the lithium cation is in closer proximity to oxygen and can assist P–O bond breaking more effectively by stabilizing the emerging alkoxide

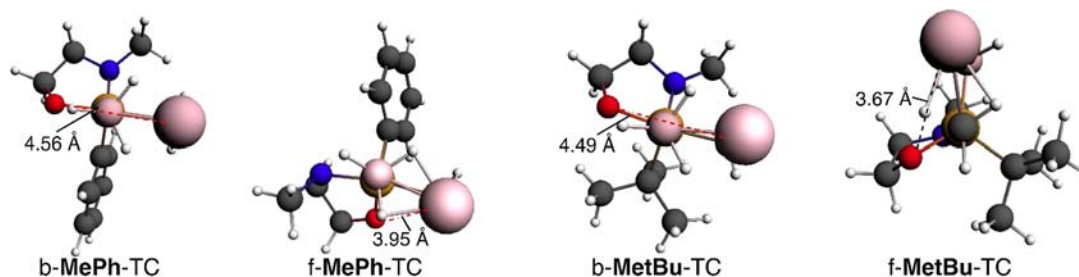
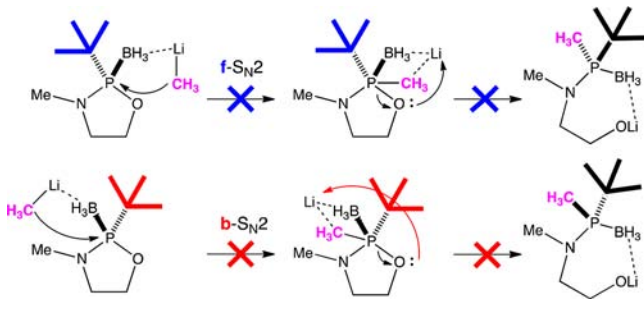


Figure 5. Computed structure (Li–O distance in Å) of the pentacoordinate TC in backside and frontside $S_N2@P$ reactions of MeLi with MePh and MetBu in toluene.

already in an earlier stage. Thus, frontside $S_N2@P$ becomes preferred over backside $S_N2@P$ in the case of MeLi + MePh.

3.4. Reactions of MetBu. The $S_N2@P$ reaction profiles for MeLi + MetBu are similar to those for MeLi + MePh (see Figure 3). In particular, the frontside $S_N2@P$ pathway remains preferred over the backside one due to the aforementioned closer proximity between oxygen and lithium, in this case ~ 0.8 Å compared to the backside pathway (see Figure 5). Yet, there is also a striking difference between the reactions of MePh and MetBu. The barrier heights go up for all elementary reaction steps along the backside as well as frontside $S_N2@P$ processes as one goes from phenyl (in MePh) to the sterically more demanding *t*-butyl substituent at P (in MetBu). Thus, both pathways become relatively less viable in the latter case (see Scheme 7). This is in line with the observation that the corresponding substrates in the experiments do not show $S_N2@P$ reactivity (see Scheme 2).

Scheme 7. Computed Backside and Frontside $S_N2@P$ Pathways of MeLi + MetBu



3.5. Reactions of HPh. As pointed out above, the BOP substrates HPh and HtBu react with a first methyl lithium molecule via facile lithiation at nitrogen. In the case of HPh, this lithiation proceeds via a barrier of <1 kcal/mol and is -53.6 kcal/mol exothermic. The formation of the encounter complex with a second methyl lithium molecule is -29.8 kcal/mol exothermic. In this complex, methyl lithium coordinates via Li to the O atom of the leaving group, while simultaneously the methyl group is in a bridging position between its own Li atom and the Li atom coordinated to N. Note that in the course of this association, the two Li atoms approach each other and achieve a short Li–Li contact of 2.49 Å (see Figure 6). This encounter complex serves either as the reactant complex from which the one-step frontside $S_N2@P$ reaction proceeds or it can be transformed via a 13 kcal/mol barrier in toluene into the 10 kcal/mol higher-energy reactant complex for the one-step backside $S_N2@P$ reaction by migrating the nucleophilic methyl group from its bridging position in between the two Li atoms entirely to the N-coordinated Li atom. Along this migration, the Li–Li bond dissociates.

The frontside $S_N2@P$ reaction proceeds via nucleophilic attack of Me at P in a sterically relatively crowded TS at nearly 55 kcal/mol above the frontside reactant complex. The path of nucleophilic attack is blocked by the Li_2 unit which, in the course of this reaction step, dissociates its relatively soft Li–Li bond (see Figure 6). Note that the pentacoordinate species is no longer a stable intermediate (or TC).

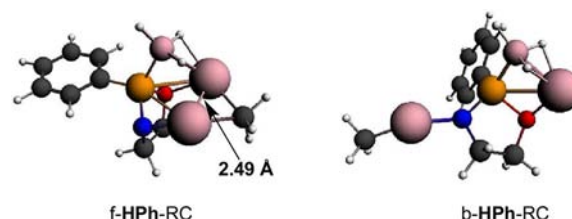


Figure 6. Reactant complexes for the frontside (encounter complex) and backside $S_N2@P$ reaction of 2 MeLi + HPh (in toluene, the former is 10 kcal/mol more stable than the latter).

The reason is that here, at variance with the reactions of the N-methylated substrates, the O atom is at any time, starting from the reactant complex, in close proximity and coordinating to Li^+ cation. Consequently, the evolving alkoxide leaving group is directly stabilized and can dissociate in a concerted manner, without the need of a separate elementary reaction step involving Li^+ migration from BH_3 to O. The result is a single-step $S_N2@P$ reaction with lithium-mediated P–O bond breaking for both the frontside pathway and the backside pathway discussed below.

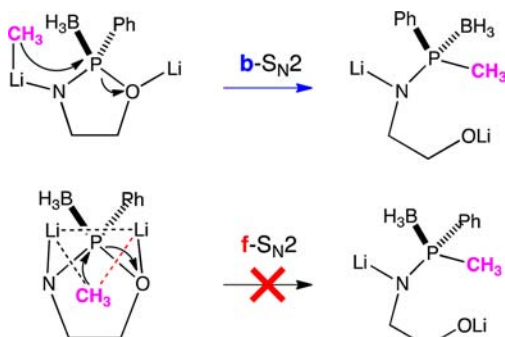
On the other hand, the backside $S_N2@P$ reaction occurs from b-HPh-RC, that is, after the Li–Li bond has already been broken. This backside reaction involves a sterically somewhat less demanding configuration in the TS which is 6.3 kcal/mol above to the backside reactant complex or 17 kcal/mol above the encounter complex f-HPh-RC. Thus, the backside pathway prevails as it is associated with two steps with relatively low barriers: (a) a methyl rearrangement from encounter complex to b- $S_N2@P$ reactant complex with a barrier of 13 kcal/mol, followed by (b) a favorable $S_N2@P$ barrier of some 6 kcal/mol (see Figure 4). Note also that now the backside pathway does not suffer from a larger distance between Li^+ and O, in contrast to the situation for the N-methylated substrates. The reason is that the Li^+ stemming from the second methyl lithium remains coordinated to BH_3 at the side of O, whereas the nucleophilic methyl can coordinate in the backside reactant complex to the other Li^+ that was incorporated in the earlier lithiation step.

3.6. Reactions of HtBu. The $S_N2@P$ mechanistic pathways for the sterically somewhat more crowded HtBu substrate are very similar to those of HPh (compare Schemes 8 and 9). The main difference is that all substitution barriers for HtBu are higher by 8–10 kcal/mol (see Figures 3 and 4). Thus, the backside $S_N2@P$ reaction still prevails and, at variance with the frontside process, is observed in the corresponding experiments.

3.7. Li Coordination to B versus O. An interesting finding of this study is that, in the reactant complex and preTS of the $S_N2@P$ reactions, the lithium of the MeLi reactant always coordinates to the B atom (or BH_3 group) of the BOP substrate and only in some cases also to O (see, e.g., Figures 6 and 7).¹⁰

The origin of this coordination behavior is found upon inspection of the electronic structure of the BOP substrate. In the first place, the formal charges in the substrate are P^+B^- . This agrees well with the fact that the highest occupied molecular orbital (HOMO) of this molecule has a large amplitude on BH_3 , larger than on O.

Scheme 8. Computed Backside and Frontside $S_N2@P$ Pathways of MeLi + HPh, Starting from Reactant Complex after Lithiation



Scheme 9. Computed Backside and Frontside $S_N2@P$ Pathways of MeLi + HtBu, Starting from Reactant Complex after Lithiation

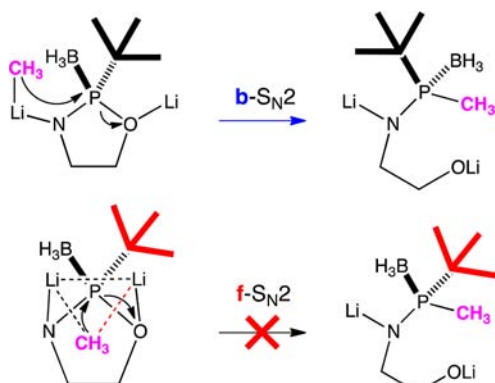


Figure 7. MeLi coordinates via Li to the BH_3 group.

Furthermore, the accumulated charge of the BH_3 group of -0.43 au (computed from the VDD atomic charges) is significantly more negative than the O atomic charge of -0.17 au (see Figure 8). The situation in related B-methylated BOP is similar (see Figure 8). In this scenario, the BH_3 group behaves as a potent directing group that strongly coordinates to the metal center of the approaching organometallic reagent.²⁰

4. CONCLUSION

In summary, we have demonstrated that the only factor that governs the stereodivergent ring-opening in 2-phenyl BOPs is the substitution at the nitrogen atom of the heterocycle. Thus, BOPs **4** and **12** react with MeLi or *o*-AnLi via backside $S_N2@P$ with inversion of configuration at phosphorus. On the other hand, N-methylated BOP (**5**) reacts via frontside $S_N2@P$, as it had been previously described by Jugé, with retention of configuration at phosphorus.

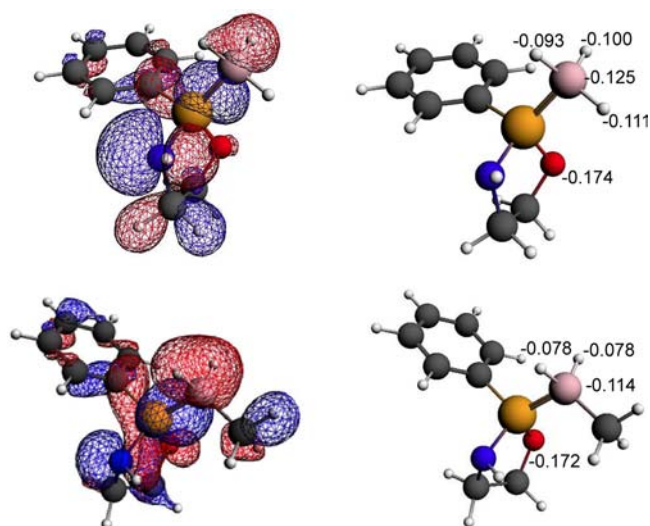


Figure 8. HOMO (left) and VDD atomic charges (in au, right) of HPh (upper) and HPh with singly methylated boron (lower).

Our DFT computations on model reactions of methyl lithium with model oxazaphospholidines yield trends in reactivity that agree well with experimental observations: The N-methylated substrate **MePh** reacts preferentially via a two-step frontside $S_N2@P$ yielding a ring-opened product in which the nucleophilic methyl binds to P with retention of configuration. Likewise **MetBu** also prefers the frontside $S_N2@P$ pathway, but all barriers involving the sterically more congested **MetBu** substrate are higher, and the corresponding substrate in experiments turns out to be unreactive. On the other hand, the substrates **HPh** and **HtBu** react with a first methyl lithium molecule via facile N-lithiation. Next, a second equivalent of methyl lithium reacts in a single step via preferential backside $S_N2@P$ substitution.

The origin of the preference for frontside substitution in the case of the N-methylated substrates **MePh** and **MetBu** is the closer proximity, in this pathway, of the Li^+ ion to the O leaving group. Proceeding from the encounter complex of the frontside pathway, the Li atom is from the beginning coordinating to BH_3 on the same side as the leaving-group O atom. Therefore, in the second reaction step, the evolving alkoxide leaving group can relatively easily access the Li^+ ion and engage in a stabilizing interaction. Along the backside pathway, the methyl lithium reagent coordinates via Li at the opposite side with respect to the O atom. Consequently, the transfer of Li^+ to the leaving group involves bridging a larger spatial separation which is associated with a higher barrier.

The preference for the backside substitution in the case of the unmethylated **HPh** and **HtBu** is the combination of thermodynamically relatively stable frontside encounter complexes of the second methyl lithium reagent with the lithium-stabilized but effectively negatively charged substrates in combination with a sterically less accessible path of approach, which is blocked by an Li_2 cluster. Furthermore, the backside pathway is not hampered anymore by a large distance between Li^+ and the evolving oxide leaving group to which this cation must migrate because of the presence of two Li^+ cations, one of which is always in close proximity to O.

■ ASSOCIATED CONTENT

■ Supporting Information

Experimental procedures, compound characterization data, and spectra for all new compounds, and CIF file for compound 9. Structural data and total energies of stationary points. This material is available free of charge via the Internet at <http://pubs.acs.org>.

■ AUTHOR INFORMATION

Corresponding Author

f.m.bickelhaupt@vu.nl; antoni.riera@irbbarcelona.org; xavier.verdaguer@irbbarcelona.org

Author Contributions

[†]These authors contributed equally.

Notes

The authors declare no competing financial interest.

■ ACKNOWLEDGMENTS

We thank The Netherlands Organization for Scientific Research (NWO-CW), the National Research School Combination-Catalysis (NRSC-C), Ikerbasque, MICINN (CTQ2011-23620, CTQ2010-16959/BQU), IRB Barcelona, and the Generalitat de Catalunya (2009SGR-00901) for financial support. T.L. thanks the Generalitat de Catalunya for a FI fellowship.

■ REFERENCES

- (1) *Phosphorous Ligands in Asymmetric Catalysis*; Börner, A., Ed.; Wiley-WCH: Weinheim, 2008; Vol. I-III.
- (2) (a) Knowles, W. S.; Sabacky, M. J.; Vineyard, B. D.; Weinkauff, D. J. *J. Am. Chem. Soc.* **1975**, *97*, 2567–2568. (b) Vineyard, B. D.; Knowles, W. S.; Sabacky, M. J.; Bachman, G. L.; Weinkauff, D. J. *J. Am. Chem. Soc.* **1977**, *99*, 5946–5952.
- (3) For reviews on P-stereogenic phosphines, see: (a) Grabulosa, A. In *P-Stereogenic Ligands in Asymmetric Catalysis*; RSC Publishing: Cambridge, 2011. (b) Grabulosa, A.; Granell, J.; Muller, G. *Coord. Chem. Rev.* **2007**, *251*, 25–90. (c) Kolodiazhyi, O. I. *Tetrahedron: Asymmetry* **2012**, *23*, 1–46.
- (4) For recent examples of the use of P-stereogenic phosphines in catalysis, see: (a) Imamoto, T.; Tamura, K.; Zhang, Z.; Horiuchi, Y.; Sugiyama, M.; Yoshida, K.; Yanagisawa, A.; Gridnev, I. D. *J. Am. Chem. Soc.* **2012**, *134*, 1754–1769. (b) Tamura, K.; Sugiyama, M.; Yoshida, K.; Yanagisawa, A.; Imamoto, T. *Org. Lett.* **2010**, *12*, 4400–4403. (c) Wang, X.; Buchwald, S. L. *J. Am. Chem. Soc.* **2011**, *133*, 19080–19083. (d) Ito, H.; Okura, T.; Matsuura, K.; Sawamura, M. *Angew. Chem., Int. Ed.* **2010**, *49*, 560–563. (e) Chen, I.-H.; Yin, L.; Itano, W.; Kanai, M.; Shibasaki, M. *J. Am. Chem. Soc.* **2009**, *131*, 11664–11665. (f) Geng, H.; Zhang, W.; Chen, J.; Hou, G.; Zhou, L.; Zou, Y.; Wu, W.; Zhang, X. *Angew. Chem., Int. Ed.* **2009**, *48*, 6052–6054. (g) Bergin, E.; O'Connor, C. T.; Robinson, S. B.; McGarrigle, E. M.; O'Mahony, C. P.; Gilheany, D. G. *J. Am. Chem. Soc.* **2007**, *129*, 9566–9567. (h) Tang, W.; Qu, B.; Capacci, A. G.; Rodriguez, S.; Wei, X.; Haddad, N.; Narayanan, B.; Ma, S.; Grinberg, N.; Yee, N. K.; Krishnamurthy, D.; Senanayake, C. H. *Org. Lett.* **2010**, *12*, 176–179. (i) Granender, J.; Secci, F.; Canipa, S. J.; O'Brien, P.; Kelly, B. *J. Org. Chem.* **2011**, *76*, 4794–4799. (j) Landert, H.; Spindler, F.; Wyss, A.; Blaser, H.; Pugin, B.; Ribourduille, Y.; Gschwend, B.; Ramalingam, B.; Pfaltz, A. *Angew. Chem., Int. Ed.* **2010**, *49*, 6873–6876. (k) Rajendran, K. V.; Gilheany, D. G. *Chem. Commun.* **2012**, *48*, 10040–10042. (l) Stankevicius, M.; Pietrusiewicz, K. M. *J. Org. Chem.* **2007**, *72*, 816–822. (m) Gatineau, D.; Giordano, L.; Buono, G. *J. Am. Chem. Soc.* **2011**, *133*, 10728–10731. (n) León, T.; Parera, M.; Roglans, A.; Riera, A.; Verdaguer, X. *Angew. Chem., Int. Ed.* **2012**, *51*, 6951–6955. (o) Revés, M.; Ferrer, C.; León, T.; Doran, S.; Etayo, P.; Vidal-Ferran, A.; Riera, A.; Verdaguer, X. *Angew. Chem., Int. Ed.* **2010**, *49*, 9452–9455.
- (5) (a) Jugé, S.; Stephan, M.; Laffitte, J. A.; Genet, J. P. *Tetrahedron Lett.* **1990**, *31*, 6357–6360. (b) Jugé, S.; Stephan, M.; Merdès, R.; Genet, J. P.; Halut-Desportes, S. *J. Chem. Soc., Chem. Commun.* **1993**, 531–533. (c) Darcel, C.; Uziel, J.; Jugé, S. Synthesis of P-stereogenic phosphorus compounds based on chiral aminoalcohols as chiral auxiliary. In *Phosphorous Ligands in Asymmetric Catalysis*; Börner, A., Ed.; Wiley-WCH: Weinheim, 2008; Vol. III, pp 1211–1233.
- (6) For other examples of the Jugé-Stephan method and related systems, see: (a) Brown, J. M.; Laing, J. C. P. *J. Organomet. Chem.* **1997**, *529*, 435–444. (b) den Heeten, R.; Swennenhuis, B. H. G.; van Leeuwen, P. W. N. M.; de Vries, J. G.; Kamer, P. C. J. *Angew. Chem., Int. Ed.* **2008**, *47*, 6602–6605. (c) Maienza, F.; Spindler, F.; Thommen, M.; Pugin, B.; Malan, C.; Mezzetti, A. *J. Org. Chem.* **2002**, *67*, 5239–5249. (d) Yang, H.; Lukan, N.; Mathieu, R. *Organometallics* **1997**, *16*, 2089–2095. (e) Leyris, A.; Nuel, D.; Giordano, L.; Achard, M.; Buono, G. *Tetrahedron Lett.* **2005**, *46*, 8677–8680. (f) Bondarev, O. G.; Goddard, R. *Tetrahedron Lett.* **2006**, *47*, 9013–9015. (g) Han, Z. S.; Goyal, N.; Herbage, M. A.; Sieber, J. D.; Qu, B.; Xu, Y.; Li, Z.; Reeves, J. T.; Desrosiers, J.; Ma, S.; Grinberg, N.; Lee, H.; Mangunuru, H. P. R.; Zhang, Y.; Krishnamurthy, D.; Lu, B. Z.; Song, J. J.; Wang, G.; Senanayake, C. H. *J. Am. Chem. Soc.* **2013**, *135*, 2474–2477.
- (7) Bauduin, C.; Moulin, D.; Kaloun, E. B.; Darcel, C.; Jugé, S. *J. Org. Chem.* **2003**, *68*, 4293–4301.
- (8) León, T.; Riera, A.; Verdaguer, X. *J. Am. Chem. Soc.* **2011**, *133*, 5740–5743.
- (9) In order to avoid steric congestion, the alkyl/aryl groups on phosphorous are placed invariably in a *trans* disposition with respect to the other substituents in the oxazaphospholidine ring, see refs 5 and 6.
- (10) For N-methylated oxazaphospholidines, Jugé and co-workers postulated that coordination of the alkyl lithium reagent to oxygen directed the frontside $S_N2@P$, see ref 5c.
- (11) (a) te Velde, G.; Bickelhaupt, F. M.; Baerends, E. J.; Fonseca Guerra, C.; van Gisbergen, S. J. A.; Snijders, J. G.; Ziegler, T. *J. Comput. Chem.* **2001**, *22*, 931–967. (b) Computer code *ADF2010.01*: Baerends, E. J.; Autschbach, J.; Bashford, D.; Bérces, A.; Bickelhaupt, F. M.; Bo, C.; Boerrigter, P. M.; Cavallo, L.; Chong, D. P.; Deng, L.; Dickson, R. M.; Ellis, D. E.; van Faassen, M.; Fan, M.; Fischer, T. H.; Fonseca Guerra, C.; Ghysels, A.; Giammona, A.; van Gisbergen, S. J. A.; Götz, A. W.; Groeneveld, J. A.; Gritsenko, O. V.; Grüning, M.; Harris, F. E.; Harris, P.; van den Hoek, P.; Jacob, C. R.; Jacobsen, H.; Jensen, L.; van Kessel, G.; Kootstra, F.; Krykunov, M. V.; van Lenthe, E.; McCormack, D. A.; Michalak, A.; Mitoraj, M.; Neugebauer, J.; Nicu, V. P.; Noodleman, L.; Osinga, V. P.; Patchkovskii, S.; Philipsen, P. H. T.; Post, D.; Pye, C. C.; Ravenek, W.; Rodriguez, J. I.; Ros, P.; Schipper, P. R. T.; Schreckenbach, G.; Seth, M.; Snijders, J. G.; Solà, M.; Swart, M.; Swerhone, D.; te Velde, G.; Vernooijs, P.; Versluis, L.; Visscher, L.; Visser, O.; Wang, F.; Wesolowski, T. A.; van Wezenbeek, E. M.; Wiesenekker, G.; Wolff, S. K.; Woo, T. K.; Yakovlev, A. L.; Ziegler, T. *SCM, Theoretical Chemistry*; Vrije Universiteit: Amsterdam, The Netherlands; <http://www.scm.com/>.
- (12) (a) Hoe, W.-M.; Cohen, A. J.; Handy, N. C. *Chem. Phys. Lett.* **2001**, *341*, 319–328. (b) Lee, C.; Yang, W.; Parr, R. G. *Phys. Rev. B* **1988**, *37*, 785–789.
- (13) (a) van Lenthe, E.; Baerends, E. J.; Snijders, J. G. *J. Chem. Phys.* **1994**, *101*, 9783–9792. (b) van Lenthe, E.; van Leeuwen, R.; Baerends, E. J.; Snijders, J. G. *Int. J. Quantum Chem.* **1996**, *57*, 281–293.
- (14) (a) Klamt, A.; Schüürmann, G. *J. Chem. Soc., Perkin Trans.* **1993**, *2*, 799–805. (b) Klamt, A. *J. Phys. Chem.* **1995**, *99*, 2224–2235. (c) Pye, C. C.; Ziegler, T. *Theor. Chem. Acc.* **1999**, *101*, 396–408. (d) Swart, M.; Rösler, E.; Bickelhaupt, F. M. *Eur. J. Inorg. Chem.* **2007**, 3646–3654.
- (15) (a) van Bochove, M. A.; Swart, M.; Bickelhaupt, F. M. *J. Am. Chem. Soc.* **2006**, *128*, 10738–10744. (b) Bento, A. P.; Bickelhaupt, F. M. *J. Org. Chem.* **2007**, *72*, 2201–2207.
- (16) Bickelhaupt, F. M.; Baerends, E. J. In: *Reviews in Computational Chemistry*; Lipkowitz, K. B., Boyd, D. B., Eds.; Wiley-VCH: New York, 2000, Vol. 15, pp 1–86.

(17) (a) Fonseca Guerra, C.; Handgraaf, J.-W.; Baerends, E. J.; Bickelhaupt, F. M. *J. Comput. Chem.* **2004**, *25*, 189–210.

(b) Bickelhaupt, F. M.; van Eikema Hommes, N. J. R.; Fonseca Guerra, C.; Baerends, E. J. *Organometallics* **1996**, *15*, 2923–2931.

(18) As a simplified model system, the aggregation of MeLi has not been taken into account. We expect the same principles, in particular, the directing effect of Li coordination to happen also in (MeLi)_n aggregates. The main effect of using MeLi instead of, e.g., (MeLi)₄, will be a less crowded situation in our model, leading to less steric repulsion and somewhat lower barriers. Importantly, this steric effect will influence the various pathways in a similar fashion and therefore is expected to have no large effect on trends.

(19) Bento, A. P.; Bickelhaupt, F. M. *Chem. Asian J.* **2008**, *3*, 1783–1792.

(20) Metal-borane interactions are known both in solid-state and in solution, see: (a) Barozzino Consiglio, G.; Queval, P.; Harrison-Marchand, A.; Mordini, A.; Lohier, J.; Delacroix, O.; Gaumont, A.; Gérard, H.; Maddaluno, J.; Oulyadi, H. *J. Am. Chem. Soc.* **2011**, *133*, 6472–6480. (b) Izod, K.; Wills, C.; Clegg, W.; Harrington, R. W. *Organometallics* **2010**, *29*, 4774–4777. (c) Izod, K.; Wills, C.; Clegg, W.; Harrington, R. W. *Organometallics* **2007**, *26*, 2861–2866. (d) Izod, K.; Wills, C.; Clegg, W.; Harrington, R. W. *Organometallics* **2006**, *25*, 38–40. (e) Kawano, Y.; Hashiva, M.; Shimoi, M. *Organometallics* **2006**, *25*, 4420–4426. (f) Müller, G.; Brand, J. *Organometallics* **2003**, *22*, 1463–1467. (g) Kakizawa, T.; Kawano, Y.; Shimoi, M. *Organometallics* **2001**, *20*, 3211–3213 and references therein.